Journal of Radiation Research, Vol. 59, No. 6, 2018, pp. 677–684
doi: 10.1093/jrr/rry063
Advance Access Publication: 15 August 2018

Measurement of ^{90}Sr radioactivity in cesium hot particles originating from the Fukushima Nuclear Power Plant Accident

Shunsuke Nakamura[1], Tsuyoshi Kajimoto[1], Kenichi Tanaka[1], Hideo Yoshida[1], Makoto Maeda[2] and Satoru Endo[1,*]

[1]Quantum Energy Applications, Graduate School of Engineering, Hiroshima University, 1-4-1 Kagamiyama, Higashi-Hiroshima 739-8527, Japan
[2]Nature Science Center for Basic Research and Development (N-BARD), Hiroshima University, 1-3-1 Kagamiyama, Higashi-Hiroshima 739-8526, Japan
*Corresponding author. Quantum Energy Applications, Graduate School of Engineering, Hiroshima University, 1-4-1 Kagamiyama, Higashi-Hiroshima 739-8527, Japan. Tel: +81-82-424-7612; Fax: +81-82-424-7619; Email: endos@hiroshima-u.ac.jp
(Received 29 November 2017; revised 15 February 2018; editorial decision 6 July 2018)

ABSTRACT

A method for the determination of $^{134+137}$Cs and ^{90}Sr in cesium hot particles (Cs-HPs) originating from the Fukushima Daiichi Nuclear Power Plant accident has been developed. The method depends on a response function that is calculated by PHITS code and fitted to the beta-ray spectrum measured with a Si-detector. The $^{134+137}$Cs radioactivity in the Cs-HPs was consistent with that measured by a Ge-detector, thus confirming the reliability of the method. The ^{90}Sr/^{137}Cs ratios, which ranged from 0.001 to 0.0042, were consistent with a ^{90}Sr/^{137}Cs inventory ratio for contaminated soil samples. That is, the extracted Cs-HPs contained ^{90}Sr in the same ratio as that for the ^{90}Sr/^{137}Cs inventory ratio for the contaminated soils. The method is attractive in that the samples are unaltered, andthat no chemical separation techniques are required.

Keywords: Fukushima Daiichi Nuclear Power Plant Accident; Cs hot particle; ^{90}Sr; Monte Carlo simulation

INTRODUCTION

The nuclear accident at the Fukushima Daiichi Nuclear Power Plant (FDNPP) was triggered by a massive earthquake and an associated tsunami on 11 March 2011. A large quantity of radioactive nuclides was released into the environment, and this resulted in severe contamination of a wide area from the southern Tohoku region to the northern Kanto region of the Honshu Island [1–3]. The dominant depositions occurred on 14–15 and 20–21 March 2011 [4].

At the Meteorological Research Institute, Adachi *et al.* conducted dust sampling from 14 March 2011. They found Cs hot particles (Cs-HPs) containing high levels of $^{134+137}$Cs on the sample collection filters [4]. Yamaguchi *et al.* reported that the major elements in the Cs-HPs were mainly Si and O. The Cs-HPs were thought to be composed of silicate glass [5] and to be water-insoluble. These are expected characteristics of Cs-HPs. In addition, it has been reported that the Cs-HPs also contained uranium, based on X-ray fluorescence analysis [6]. This indicates that the Cs-HPs did not selectively adsorb $^{134+137}$Cs; thus, it is possible that the Cs-HPs contain various types of fission products [3]. The short half-life radionuclides would have already decayed to insignificant amounts due to the passing of >7 years since the FDNPP accident. However, long-half-life radionuclides remain in the environment. As an example, ^{90}Sr has a half-life of 29.1 years, which is comparable with the 30.0-year half-life of ^{137}Cs.

The Ministry of Education, Culture, Sports, Science and Technology (MEXT) conducted a 2 km grid contamination study from June to August 2011 [7]. In the MEXT study, ^{90}Sr radioactivity was detected in soil samples [7]. However, there are no reports about ^{90}Sr radioactivity in Cs-HPs. ^{90}Sr is well known to be soluble in water; hence, ^{90}Sr contamination could be expected to spread deep into the ground soil [8]. In contrast, Cs-HPs are insoluble in water, so ^{90}Sr present inside a Cs-HP will not spread deep into the soil. Thus, ^{90}Sr contained within Cs-HPs would display different physical behavior in terms of mobility in the soil. As a result, the measurement of ^{90}Sr radioactivity in Cs-HPs is important for understanding the dynamics of ^{90}Sr in the environment.

A chemical separation technique is normally used to monitor ^{90}Sr radioactivity in soil. However, Cs-HPs are quite small, making it difficult to extract ^{90}Sr from them. Furthermore, chemical separation is a destructive procedure, and the Cs-HP samples would not be able to be investigated further after the chemical separation. In this research, radiometric determination of the ^{90}Sr in Cs-HPs is proposed without the use of chemical separation. In this method, beta-rays emitted from the Cs-HPs were measured using a Si-detector. The radioactivities of $^{134+137}$Cs and ^{90}Sr were then determined by fitting the calculated response functions to the measured beta-ray spectrum. This method was intended for Cs-HPs.

MATERIALS AND METHODS

Soil samples

Soil sampling was performed from 30 October to 3 November 2013. Eleven soil cores were taken at a total of 11 locations in Namie Town, Futaba Town and Minami-Soma City. The radius and the depth of the soil cores were 2.5 and 30 cm, respectively. The sampling points are shown on the map in Fig. 1. The soil cores were divided into seven layers (0–5 cm: two layers of 2.5 cm thickness, 5–30 cm: five layers of 5 cm thickness). Each sample layer was dried in an oven for ~17 h prior to measurement by a coaxial type Ge-detector (GMX-30200-P; Ortec) [9]. Given that the Cs-HPs may not penetrate deep into the soil layers because of their relative insolubility in water, the surface soils of each core were used for Cs-HP extraction. The GPS coordinates, sample IDs, and ^{134}Cs and ^{137}Cs inventories (kBq/m^2) decay-adjusted on 1 November 2013 for each location are summarized in Table 1 (see next section). These data were used to determine how much Cs-HPs contribute to the inventories of ^{134}Cs, ^{137}Cs and ^{90}Sr contained in the total contamination.

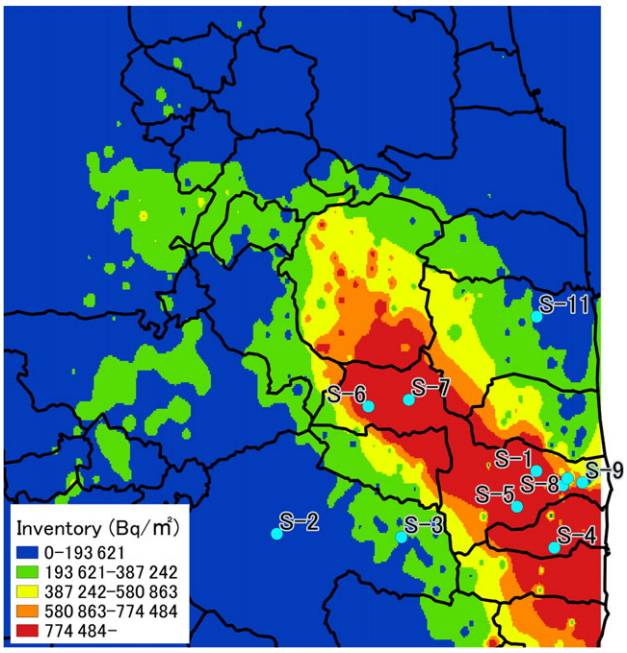

Fig. 1. Sampling points. The color chart shows the soil ^{137}Cs inventory (in Bq/m^2) obtained by MEXT [5].

Extraction of Cs-HPs from soil samples

The Cs-HPs were identified using an imaging plate (IP: BAS-MS 2040, Fujifilm). The Cs-HPs appear as a spot on a readout distribution of an IP [10]. Thirty to forty grams of soil sample was uniformly spread across a polyethylene bag, with an approximate thickness of ≤0.6 mm. The IP was placed over the polyethylene bag and exposed for 5 min. The Cs-HPs were revealed as large spots with high intensity on the readout distribution of the exposed IP. The number of Cs-HPs in the soil was counted using an image-processing technique. First, the readout of the IP was binarized with a threshold that was obtained from two standard deviations of the intensity for the background region. The sum of the mean intensity and two standard deviations of the intensity of the background region was defined as the threshold for binarizing processing. The background region was defined as the region that did not include a large spot. Second, a spot that consisted of more than six consecutive pixels was selected and counted. However, there was a possibility that the soil shielded radiation emanating from the Cs-HPs. Thus, the exposure and discrimination processes were repeated 10 times by mixing and respreading the soil. The numbers of Cs-HPs in the soil sample were obtained from the mean numbers of spots for 10 measurements.

The number of Cs-HPs in the soil samples and the amount of radioactivity in the soil samples are listed in Table 1. Cs-HP spots were observed at six locations. The Cs-HPs were limited to those spots having radioactivity of a few becquerels or more. Samples S-4 and S-5 were heavily contaminated (>10 000 kBq/m^2); however, the numbers of Cs-HP in these samples were lower than those for S-1 and S-8.

The Cs-HPs were extracted using the IP and a Geiger–Muller (GM) survey meter (IGS-133, Aloka Co, Ltd). The positions of the Cs-HPs in the polyethylene bag were determined based on the readout distribution of the exposed IP. For each region of soil that contained an identified Cs-HP spot, a small amount of soil containing the Cs-HP was separated from the bulk sample. The amount of soil around the Cs-HPs was reduced by repeating this procedure. The procedure was repeated >10 times, making sure that the particles selected did emit radiation by first checking with a collimator and GM survey meter. Six Cs-HPs, designated particles A–F were removed from the soil samples S-1 (A) and S-8 (B–F). The extracted Cs-HPs were analyzed by a Ge-detector and energy-dispersive X-ray spectrometry to confirm that their characteristics were the same as Cs-HPs in previous papers.

Gamma-ray measurement of Cs-HPs

Gamma-ray from the selected Cs-HPs was measured for 80 000 s by a well-type Ge-detector (GWL 120230-S, Seiko EG&G) that was shielded by lead of thickness 20 cm and used plastic scintillators as an anti-coincidence system for reducing the cosmic ray background [11]. The well-type Ge-detector was calibrated with soil samples for which ^{134}Cs and ^{137}Cs concentrations were obtained using a

Table 1. Sample ID, GPS coordinates, inventory (kBq/m^2) on 1 November 2013, and the number of Cs-HPs

Sample ID	GPS coodinates		Inventory (kBq/m^2)		$^{134}Cs/^{137}Cs$	No. of Cs-HPs
	Longitude	Latitude	^{137}Cs	^{134}Cs		
S-1	37.49948	140.9531697	6500	2090	0.32	5
S-2	37.43997306	140.6440781	36	16	0.43	
S-3	37.43677	140.7924264	53	22	0.42	
S-4	37.42681	140.974575	11 000	4660	0.42	1
S-5	37.46567139	140.9300531	15 800	6757	0.43	2
S-6	37.56071306	140.753175	1540	661	0.43	1
S-7	37.56707139	140.8013081	2840	1230	0.43	2
S-8	37.48580806	140.9845297	3070	1220	0.4	18
S-9	37.48852972	141.0078614	124	52	0.42	
S-10	37.49258639	140.99019	30	12	0.38	
S-11	37.64527472	140.9534778	139	60	0.43	

COAX-type Ge-detector (GMX-30200-P, ORTEC), including the sum correction [12]. The error found during calibration was estimated at 5%. Figure 2 shows an example of the gamma-ray spectrum of a Cs-HP. The 0.605, 0.796 and 0.662 MeV gamma rays of ^{134}Cs and ^{137}Cs were clearly identified, and these gamma-rays were used for ^{134}Cs and ^{137}Cs determination. The radioactivity from a single Cs-HP had quite a high counting rate for gamma-rays, confirming that the extracted particle contained radioactive Cs. The measured radioactivities of ^{134}Cs and ^{137}Cs are listed in Table 2. The radioactivity ratio of $^{134}Cs/^{137}Cs$ and the radioactivity of ^{137}Cs in Cs-HPs was reported to be 0.93–1.18 and approximately 1 to 10^5 Bq, respectively, in previous reports [4, 6, 13, 14]. Our measured radioactivity values were consistent with these reports. Particle D had high Cs radioactivity.

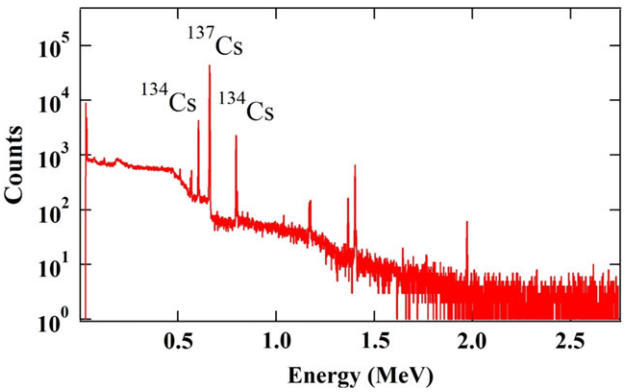

Fig. 2. Measured gamma-ray spectrum of sample A using a well-type Ge-detector.

Scanning electron microscopy and energy-dispersive X-ray spectrometry measurement

Cs-HPs were analyzed by scanning electron microscopy (SEM; S-5200, Hitachi High-Technologies Corp.) and energy-dispersive X-ray spectrometry (EDS; Genesis XM2, EDAX Japan) to obtain the shape and size of the Cs-HPs and the element compositions. This information was used in the response function calculation as described below. For SEM and EDS analyses, the extracted Cs-HPs were mounted on carbon tape and coated by vapor deposition of carbon. The SEM and EDS analyses were carried out at the Cryogenics and Instrumental Analysis Division, Natural Science Center for Basic Research and Development (N-BARD), Hiroshima University. The results of SEM and EDS analyses for particle A are shown in Fig. 3. From Fig. 3a, it can be seen that particle A is spherical with a diameter of 60 μm. Some crater-like structures are

Table 2. Radioactivity of Cs-HPs obtained using a well-type Ge-detector (15 March 2011)

Soil sample	ID	^{134}Cs (Bq)	^{137}Cs (Bq)
S-1	A	13.14 ± 0.096	14.91 ± 0.75
S-8	B	22.13 ± 1.15	24.31 ± 1.22
	C	9.21 ± 0.67	10.05 ± 0.50
	D	70.15 ± 4.98	67.95 ± 3.40
	E	4.19 ± 0.32	3.64 ± 0.18
	F	7.69 ± 0.57	8.05 ±0.40

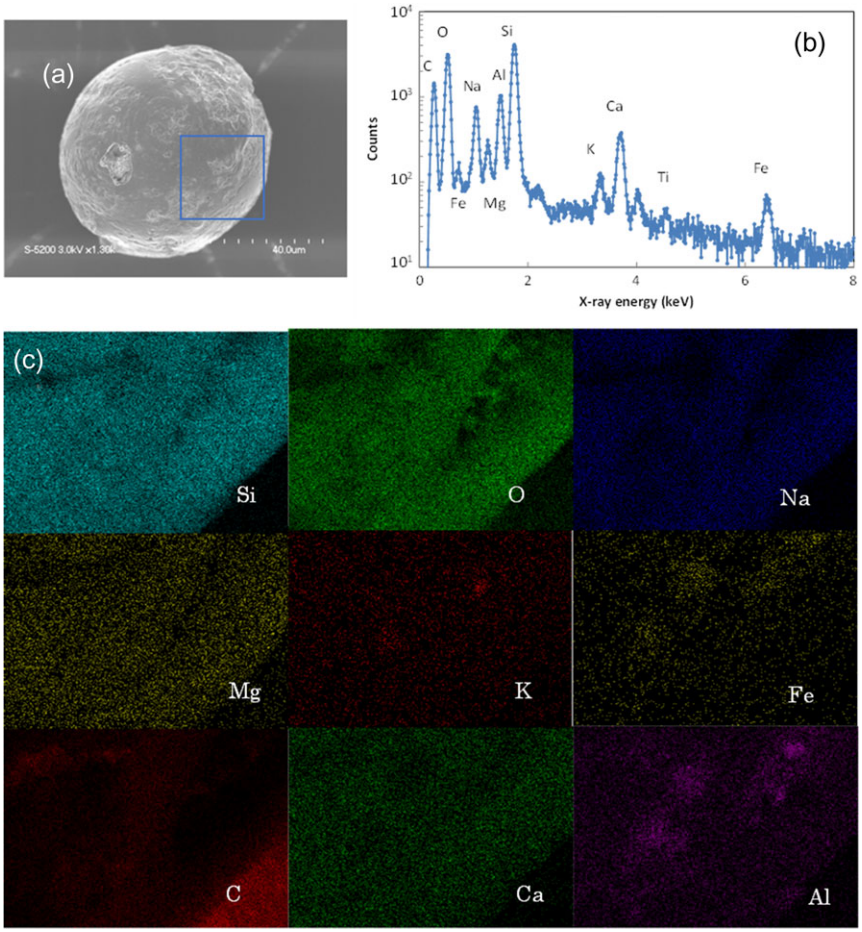

Fig. 3. (a) SEM image for Cs-HP, (b) EDS spectrum for Cs-HP and (c) element mapping at the enclosed region of (a).

present on the surface. The element composition of the particle is dominated by Si and O, but minor/trace amounts of Na, Mg, Al, K, Ca and Fe can be identified from inspection of the EDS spectrum in Fig. 3b. The major components of particle A are consistent with a previous report by Satou *et al.* [13]. Regarding the results of elemental mapping in Fig. 3c, the elements were uniformly distributed on the Cs-HP surface. Further, SEM and EDS analyses conducted on other Cs-HPs gave similar results to that of particle A. The radii of the Cs-HPs were all within the range of 20–60 μm. The average particle radius was ~40 μm.

Beta-ray measurement of Cs-HPs

Beta-rays emitted from the extracted Cs-HPs were measured using a surface-barrier-type Si-detector (CL-015-150-300, ORTEC) for 1 000 000 s. The Si-detector was shielded by 5 cm-thick lead blocks to reduce cosmic ray background. A background spectrum was also measured without the Cs-HP for 1 000 000 s. Examples of the measured spectra with and without the Cs-HP are shown in Fig. 4. The abscissa in Fig. 4 was calibrated based on the internal conversion electron from ^{137}Cs. As a result, the energy width of one channel of used analyzer corresponded to 0.7 keV. The spectrum for the Cs-HP is formed by energy deposition from beta-rays and internal conversion electrons. The energy depositions by beta-rays and internal conversion electrons are represented by the continuous and transient portions of the Cs-HP spectrum. The two peaks obtained

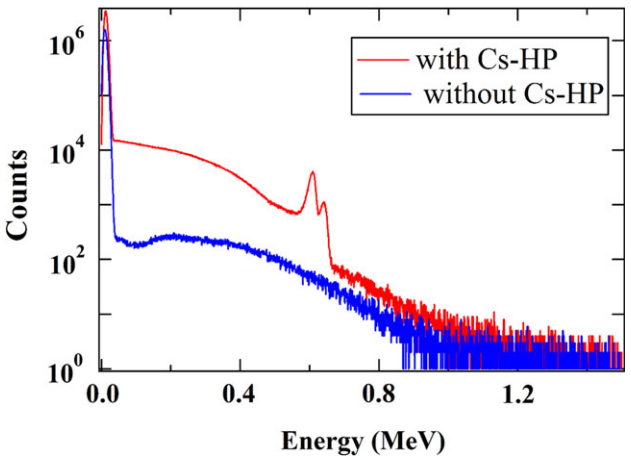

Fig. 4. Measured beta-ray spectra with and without Cs-HP (particle A).

at 0.624 and 0.656 MeV were attributable to internal conversion electrons originating from the K and L shells for ^{137}Cs. This result indicated the Cs-HP contained ^{137}Cs, which was consistent with results obtained by the Ge-detector. The count ratio of spectra with and without the Cs-HP was ~100 at 0.1 MeV and ~3 at 0.8 MeV. The counts that exceeded 1 MeV originated from beta-rays from ^{90}Y. There are three reason for that. The first reason is that the beta-ray end-point energy of ^{137}Cs is 1.18 MeV. The second reason is that gamma-rays measurement do not identify any gamma-rays emitted from radionuclides, except for ^{134}Cs and ^{137}Cs. The third reason is that, of the radionuclides released in the FDNPP accident, the radionuclide emitting only beta-rays is ^{90}Sr-^{90}Y. The beta-ray spectra for particles A–F were obtained by subtraction of the spectrum without the Cs-HP from the spectrum with the Cs-HP. The result is equal to the energy distribution deposited in the depletion layer of the Si-detector during measurement.

Response function calculation of the Si-detector

The response function, which is defined by the energy deposition probability spectrum of the depletion layer of the Si-detector for one disintegration of a source nuclide, was calculated using the Particle and Heavy Ion Transport Code System (PHITS) [15]. The measurement set-up is modeled based on the following calculation geometry: (i) the Si-detector depletion layer, dead layer and, gold electrode were modeled by columns of thicknesses of 370 µm, 2 µm and 10 nm, respectively; (ii) the detector housing was modeled by a stainless steel cylinder whose internal and external radii were 7.2 and 11.8 mm, respectively; and (iii) a lead shielding box was taken into account for this calculation. The current thickness of the depletion layer and the dead layer of the Si-detector were not determined. The response function was calculated for cases of thicknesses of 300–400 µm and 0.1–5 µm, respectively. The previously mentioned thicknesses were selected from these values. The reason for selecting this value is given in the next subsection. From the SEM and EDS results, the Cs-HP was assumed to be a spherical silicate glass of radius 40 µm. A uniform distribution of source nuclides was assumed within the Cs-HP. The response functions were calculated for ^{134}Cs, ^{137}Cs and ^{90}Sr and obtained as $f_{134}(E)$, $f_{137}(E)$ and $f_{Sr}(E)$, respectively. Their units were 1/Bq. Given that radioactive equilibrium between ^{90}Sr and ^{90}Y is realized in a few weeks, the response function of ^{90}Sr: $f_{Sr}(E)$ was calculated using the ^{90}Sr-^{90}Y equilibrium spectrum. Beta-ray energy distributions were reproduced according to reference [16]. The emission probabilities obtained from the chart of nuclides database of the National Nuclear Data Center (NNDC 2017) [17] were applied for the generation of internal conversion electrons from ^{134}Cs and ^{137}Cs. The energy distributions of beta-rays and internal conversion electrons from ^{134}Cs, ^{137}Cs and ^{90}Sr are shown in Fig. 5.

The $^{134+137}$Cs response function $f_{Cs}(E_i)$ was obtained using the radioactivity measured by the Ge-detector as:

$$f_{Cs}(E_i) = \frac{A_{134}}{A_{134} + A_{137}} \cdot f_{134}(E_i) + \frac{A_{137}}{A_{134} + A_{137}} \cdot f_{137}(E_i), \quad (1)$$

where the values of A_{134} and A_{137} are the respective radioactivities of ^{134}Cs and ^{137}Cs. The response function of $^{134+137}$Cs was normalized as 1 Bq-$^{134+137}$Cs. The calculated response functions of particle A are shown in Fig. 6. A beta-ray and internal conversion electron emitted from the Cs-HPs were moderated by the dead layer, the Cs-HP itself and so on until arrival at the depletion layer. Therefore, the transient peak signals due to internal conversion electrons were relatively broad in comparison with that of the source spectrum as shown in Fig. 6.

Determination of radioactivity of ^{90}Sr in Cs-HPs

The radioactivities of $^{134+137}$Cs and ^{90}Sr-^{90}Ywere determined by fitting the response functions for ^{90}Sr and $^{134+137}$Cs to the beta-ray spectrum measured using the Si-detector. The least squares fitting method was used. The method minimized the χ_ν^2 of:

$$\chi_\nu^2 = \frac{1}{\nu} \sum_{i=1}^{n} \frac{\{N(E_i) - [a_{Sr} \cdot f_{Sr}(E_i) + a_{Cs} \cdot f_{Cs}(E_i)]\}^2}{\sigma_i^2 + \sigma'^2_i}, \quad (2)$$

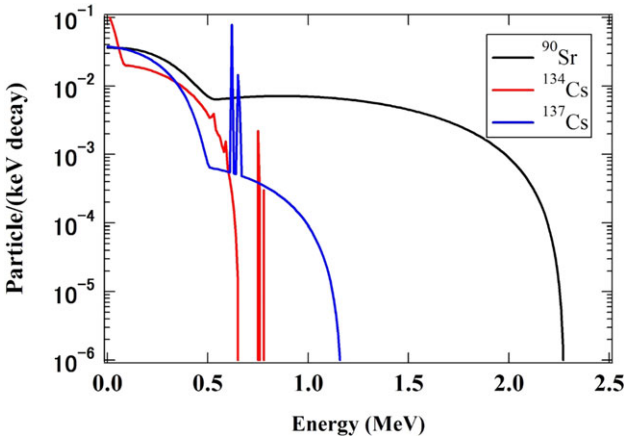

Fig. 5. Input beta-ray energy spectra for ^{134}Cs, ^{137}Cs and ^{90}Sr-^{90}Y.

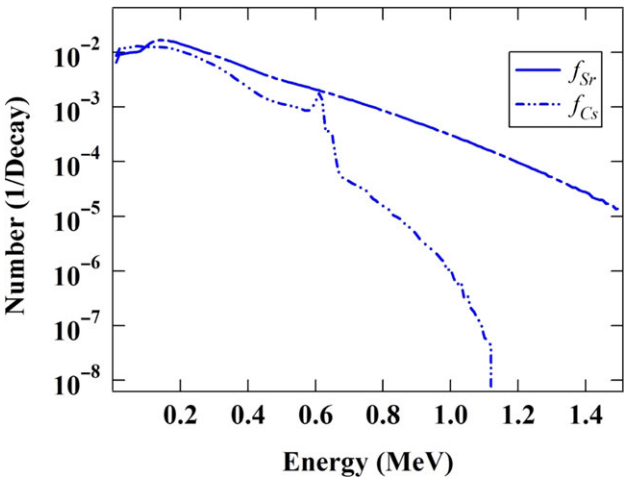

Fig. 6. Calculated response functions for radioactive Cs and ^{90}Sr.

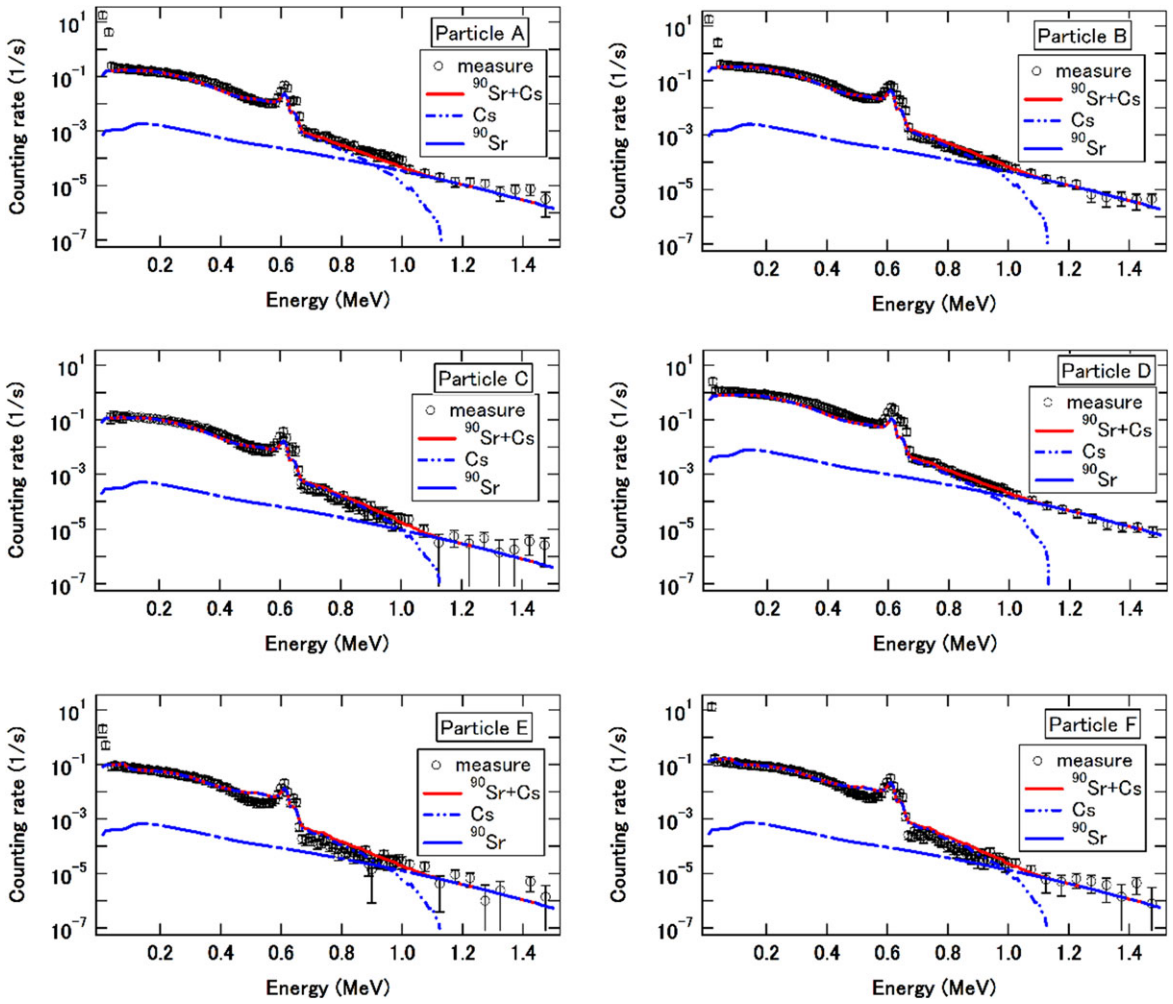

Fig. 7. The measured and calculated beta-ray spectra. The calculated beta-ray spectrum was the sum of each response function multiplied by the fitting parameter.

where E_i is the i-th energy bin of the beta ray spectrum, ν is the number of degrees of freedom, σ_t is the statistical error and σ_t' is the systematic error. The fitting parameters a_{Cs} and a_{Sr} correspond to the radioactivities of $^{134+137}$Cs and ^{90}Sr-^{90}Y, respectively. The best thicknesses for the depletion and the dead layers of the Si-detector were selected as the values that provided a response function with minimal χ_ν^2. The systematic error was estimated from a comparison with measured and calculated beta-ray spectra by using a standard ^{90}Sr source (No. 2309, Japan Radioisotope Association). The systematic error was 30%, based on the difference between the measured and calculated spectra.

RESULTS AND DISCUSSION

Fitting of beta-ray spectra by response function

The beta-ray spectra of Particles A–F and the spectra fitted by $f_{Cs}(E_i)$ and $f_{Sr}(E_i)$ are shown in Fig. 7. Note that the size of the data bin was every 0.01 MeV under 1 MeV and every 0.05 MeV above 1 MeV to reduce the number of data points having a negative value. The energy region set for fitting was from 0.05 to 1.5 MeV. The peak at 0.03 MeV was due to electrical noise; hence, this region was excluded from the fitting. The reduced χ_ν^2 values were 0.5 to 1.4.

After consideration of the fitting results, it was clear that the energy deposition above 0.9 MeV could not be explained by beta-rays from $^{134+137}$Cs alone. Beta-rays from ^{90}Sr were necessary to produce the shape of the spectrum. This indicated that the Cs-HPs contained trace levels of ^{90}Sr. The $^{134+137}$Cs and ^{90}Sr-^{90}Y radioactivities determined by fitting (decay corrected as of 1 October 2016) are summarized in Table 3. For comparison, the $^{134+137}$Cs data obtained by the Ge-detector are also listed. The radioactivities of $^{134+137}$Cs obtained by the Ge- and Si-detectors showed good agreement with each other, confirming that the determination of radioactivity by fitting the response functions to the beta-ray spectrum was a valid method. The ^{90}Sr-^{90}Y radioactivities of the extracted Cs-HPs ranged from 0.01 to 0.43 Bq.

The ^{90}Sr/^{137}Cs ratios of the Cs-HP ranged from 0.001 to 0.0042 (average value: 0.0025 ± 0.001).

In the MEXT investigation, there were four measurement points within 5 km of the S-8 sampling point. The ^{90}Sr/^{137}Cs ratios in this

Table 3. Radioactivities of samples obtained by fitting a beta-ray response function to measured spectra and measurements of Ge-detector (1 October 2016)

ID	Measurements by the Ge detector	Measurements by the Si detector		
	$^{134+137}$Cs (Bq)	$^{134+137}$Cs (Bq)	^{90}Sr-^{90}Y (Bq)	^{90}Sr/^{137}Cs
A	15.15 ± 0.67	13.59 ± 0.56	0.109 ± 0.014	0.0042 ± 0.0006
B	24.81 ± 1.10	24.77 ± 0.93	0.124 ± 0.013	0.0029 ± 0.0003
C	10.26 ± 0.45	9.85 ± 0.07	0.018 ± 0.007	0.0010 ± 0.0004
D	70.61 ± 3.08	84.19 ± 2.97	0.428 ± 0.026	0.0036 ± 0.0003
E	3.85 ± 0.17	3.26 ± 0.14	0.012 ± 0.004	0.0019 ± 0.0006
F	8.27 ± 0.37	4.98 ± 0.21	0.028 ± 0.005	0.0020 ± 0.0004

area have been reported as averaging 0.0013 ± 0.0006 over four locations, and having a maximum value of 0.0023 (decay corrected as of 1 October 2016) [7]. This value is almost identical to the values for the Cs-HPs.

Estimation of Cs-HP contribution to soil contamination

The average ^{137}Cs radioactivity of the Cs-HPs extracted from S-8 was 22.8 ± 0.7 Bq. The error is derived from the error in the ^{137}Cs radioactivities shown in Table 2. The numerical density of the Cs-HPs was calculated by dividing the number of Cs-HPs by the cross-sectional area of the soil core. If all of the 18 Cs-HPs for the S-8 soil had the same value as the average radioactivity, the ^{137}Cs inventory due to Cs-HPs can be calculated by multiplying the numerical density (9167 particles/m^2) by the average radioactivity (22.8 Bq); the estimated ^{137}Cs inventory value was 209 kBq/m^2. This value of 209 kBq/m^2 is much smaller than the total soil inventory of 3070 kBq/m^2 as specified in Table 1. The ratio of the ^{137}Cs inventory due to Cs-HPs to the total soil inventory is 0.06. In other words, the Cs-HP contribution represents ~7% of the total ^{137}Cs inventory in the soil. Cs-HPs were extracted in clear order on readout IP, which is expected to have greater radioactivity. Given that the extracted Cs-HPs have high radioactive among Cs-HPs in soil samples, the average ^{137}Cs radioactivity of the Cs-HPs may have been overestimated. Even using this overestimated value, the Cs-HP contribution was quite small. This result showed that the Cs-HPs were not the main components of soil contamination in terms of ^{137}Cs and ^{90}Sr.

A chemical separation technique is often used for the estimation of ^{90}Sr in soil samples. In such an approach, samples are dissolved in a chemical solvent for separation purposes prior to radiochemical measurement. Such dissolution of the sample constitutes a destructive analysis. In contrast, the present method has the advantage that the sample is unaltered. Thus, samples may be analyzed further after the measurement of ^{90}Sr.

CONCLUSIONS

The radioactivities of $^{137+134}$Cs and ^{90}Sr in Cs-HPs were obtained by fitting a response function of a Si-detector calculated by PHITS code to a beta-ray spectrum measured by using a Si-detector. The obtained $^{134+137}$Cs radioactivities of the Cs-HPs were consistent with those measured by a Ge-detector, thus demonstrating the reliability of the method. The results also indicated that the Cs-HPs contained ^{90}Sr. The ^{90}Sr radioactivity and ^{90}Sr/^{137}Cs ratios obtained ranged from 0.01 to 0.43 Bq and 0.001 to 0.0042, respectively. The present method has the advantage of being non-destructive and is simple in comparison with those methods based on conventional chemical separations.

ACKNOWLEDGEMENTS

The authors thank Mr Kiyoshi Nanasawa of Nippon Hoso Kyokai (NHK; Japan Broadcasting Corporation) for providing the soil samples. The Ge measurements were performed at the Radiation Laboratory, Graduate School of Engineering, Hiroshima University. The authors are grateful to the laboratory staff. The authors are also grateful to Professor Chary Rangacharulu (the University of Saskatchewan) for his advice. This work was presented at the Hiroshima International Symposium, the 2017 Fall Meeting of the Atomic Energy Society of Japan, and the 2016 Meeting of the Atomic Energy Society of Japan, Chugoku Shikoku branch.

CONFLICT OF INTEREST

The authors report that there are are no conflicts of interest.

FUNDING

This research was supported by the Japan Society for the Promotion of Science KAKENHI Grant No. JP26550031 (April 2014–March 2017).

REFERENCES

1. International Atomic Energy Agency (IAEA). *The Fukushima Daiichi Accident, Technical Volume 1: Description and Context of the Accident.* http://www-pub.iaea.org/books/IAEABooks/10962/The-Fukushima-Daiichi-Accident (1 February 2018, date last accessed).
2. United Nations Scientific Committee on the Effects of Atomic Radiation (UNSCEAR). Sources, Effects and Risks of Ionizing Radiation. UNSCEAR 2013 Report, Volume I. Report to the General Assembly with Scientific Annexes A: Levels and effects of radiation exposure due to the nuclear accident after the 2011 Great East–Japan Earthquake and Tsunami. http://www.

unscear.org/docs/publications/2013/UNSCEAR_2013_Report_Vol.I.pdf (6 February 2018, date last accessed)
3. Nuclear Emergency Response Headquarters of Japanese Government. Report of Japanese Government to the IAEA Ministerial Conference on Nuclear Safety – The accident at TEPCO's Fukushima Nuclear Power Stations. http://japan.kantei.go.jp/kan/topics/201106/iaea_houkokusho_e.html (6 February 2018, date last accessed)
4. Adachi K, Kajino M, Zaizen Y et al. Emission of spherical cesium-bearing particles from an early stage of the Fukushima nuclear accident. *Sci Rep* 2013;3:2554.
5. Yamaguchi N, Mitome M, Akiyama-Hasegawa K et al. Internal structure of cesium-bearing radioactive microparticles released from Fukushima nuclear power plant. *Sci Rep* 2016;6:20548.
6. Abe Y, Iizawa Y, Terada Y et al. Detection of uranium and chemical state analysis of individual radioactive microparticles emitted from the Fukushima Nuclear Accident using multiple synchrotron radiation X-ray analyses. *Anal Chem* 2014;86:8521–5.
7. Nuclear Regulation Authority (NRA), Japan. *The Investigation Regarding the Distribution of Radioactive Substances*. http://radioactivity.nsr.go.jp/ja/list/338/list-1.html (7 February 2018, date last accessed)
8. Korobova M E, Ermakov A, Vitaly L. ^{137}Cs and ^{90}Sr mobility in soils and transfer in soil–plant systems in the Novozybkov distinct affected by the Chernobyl accident. *Appl Geochem* 1998;13:803–14.
9. Endo S, Kimura S, Takatsuji T et al. Measurement of soil contamination by radionuclides due to Fukushima Daiichi Nuclear Power Plant accident and associated cumulative external dose estimation. *J Environm Radioact* 2012;111:18–27.
10. Mukai H, Hatta T, Kitagawa H et al. Speciation of radioactive soil particles in the Fukushima contaminated area by IP autoradiography and microanalyses. *Environ Sci Technol* 2014;48:13053–9
11. Shizuma K, Fukami K, Iwatani K et al. Low-background shielding of Ge detectors for the measurement of residual ^{152}Eu radioactivity induced by neutrons from the Hiroshima atomic bomb. *Nucl Instrum Methods Phys Res B* 1992;66:459–64.
12. Endo S, Kajimoto T, Shizuma K. Paddy-field contamination with ^{134}Cs and ^{137}Cs due to Fukushima Daiichi Nuclear Power Plant accident and soil-to-rice transfer coefficients. *J. Environm. Radioact* 2013;116:59–64.
13. Satou Y, Sueki K, Sasa K et al. First successful isolation of radioactive particles from soil near the Fukushima Daiichi Nuclear Power Plant. *Anthropocene* 2016;14:71–6.
14. Satou Y, Sueki K, Sasa K et al. Analysis of two forms of radioactive particles emitted during the early stages of the Fukushima Dai-ichi Nuclear Power Station accident. *Geochem J* 2018;52:137–43.
15. Sato T, Niita K, Matsuda N et al. Particle and Heavy Ion Transport Code System PHITS, Version 2.52. *J Nucl Sci Technol* 2013;50:913–23.
16. Endo S, Tanaka K, Kajimoto T et al. Estimation of β-ray dose in air and soil from Fukushima Daiichi Power Plant accident. *J Radiat Res* 2014;55:476–83.
17. National Nuclear Data Center. Interactive Chart of Nuclides http://www.nndc.bnl.gov/chart/ (12 February 2017, date last accessed).